WILEY

Microstructure evolution in flow formed IN 718 products and subsequent fatigue crack growth properties

M.R. Bache[1] 🆔 | C. Coleman[1] | M.P. Coleman[1] | V. Gray[1] | C. Boettcher[2]

[1] Institute of Structural Materials, College of Engineering, Swansea University, Bay Campus, Swansea SA1 8EN, UK

[2] Rolls-Royce plc, P.O. Box 31, Derby DE24 8BJ, UK

Correspondence
M. R. Bache, Institute of Structural Materials, College of Engineering, Swansea University, Bay Campus, Swansea, SA1 8EN, UK.
Email: m.r.bache@swansea.ac.uk

Abstract

With the drive towards cost-effective routes for the manufacture of engineering components, flow forming technologies are now under consideration for the production of structural axisymmetric geometries such as tubes and cones. This near net shape process is known to offer improvements in material utilisation when compared with traditional processes where substantial final machining is required. The microstructure, evolved as a result of the flow forming process together with subsequent heat treatments, will govern associated mechanical properties. Laboratory measurements of the structure-property relationships of flow formed material can be problematic, mainly because of the restrictions imposed on the extraction of conventional specimen geometries since most of the finished tubular or cone structures will contain thin and curved walls. The development of a suitable specimen design and associated test technique for the measurement of fatigue crack growth rates at room and elevated temperatures is presented. Data obtained from flow formed Inconel 718 (IN 718) will be compared with specimens of the exact same geometry but machined from conventionally forged IN 718 stock. This allowed for validation of the novel flow formed test in addition to an assessment of the damage tolerance of the flow formed variant. The intimate relationship between local microstructure and fracture mechanisms will be described.

KEYWORDS
crack propagation, nickel-based alloys, test development, manufacturing

1 | INTRODUCTION

Tubular structures for gas turbine engines are typically produced by machining to the final form from over-size solid forgings or ring rolled preforms. This can prove to be an expensive route to market, in particular generating a high volume of waste material and resulting in a low "buy to fly ratio", ie the ratio between stock material and that which eventually enters service. In contrast, flow forming could offer a more cost-effective manufacturing option for the production of near net shape cylindrical

---

Nomenclature: da/dN, crack growth rate (m/cycle); ΔK, stress intensity range per cycle (MPa$\sqrt{\text{m}}$); EBSD, electron backscattered diffraction; FCG, fatigue crack growth

and conical structures. Final machining of such parts is normally restricted to mating flanges and cooling features. Thus, material sustainability is improved plus the cold forming process itself consumes lower energy and tooling expense whilst increasing the rate of component production and reducing supplier lead times.

The ambient temperature flow forming method uses a configuration of rollers to apply compressive forces on the external diameter of a cylindrical preform mounted on a rotating mandrel. Because of the resultant, spiralling, contact with the rollers, the wall thickness of the preform is reduced, initiating a coincident increase in length along the mandrel. The localised compressive force applied during the process results in a combination of axial and radial strain, causing material to flow plastically in 3-dimensional space.[1] The localised nature of the incremental deformation during flow forming is such that the deformation is constrained by the surrounding non-deformed elastic material to one side and plastically deformed but now elastic material to the other. This leads to an inhomogeneous material flow between the roller and the preform surface, giving rise to complex evolution of stress and strain during the process.[2,3] The resultant cold work enhances yield and tensile strength, hardness, and fatigue strength.

The post-processing properties can then be customised through heat treatment, with a variety of reports addressing a range of materials and different degrees of flow formed wall reduction.[4-7] Amongst these studies, laboratory-scaled research plus full-scale production trials have been conducted to optimise key process parameters relating to the various material systems, discussed in particular in previous references.[3,7]

Notably, IN 718 has long been a workhorse material particularly in gas turbine engines where moderate strength is retained at temperatures approaching 650°C. Owing to the proprietary nature of specific components, detailed descriptions of flow formed structures proposed

for future aero-engine designs together with optimisation of the associated process variables may not be discussed in detail. Instead, the present paper will concentrate on the microstructure evolution in IN 718 when subjected to typical flow forming routines.

Measurement of fundamental mechanical properties of flow formed IN 718 material, in particular the fatigue crack growth (FCG) response, will also be described. It is important to define and understand the effects of the flow forming process on subsequent damage tolerance characteristics. In particular, comparisons to FCG behaviour measured in conventional forms of IN 178 are essential to support component design and lifing activities. However, evaluating such mechanical properties in the laboratory setting can be difficult as conventional scale test pieces may not be easily extracted from relatively thin and curved flow formed sections. The design of appropriate, novel specimens and associated test techniques will be described together with assumptions made when analysing the crack growth characteristics. Detailed fractography will identify the predominant mode of interaction between the advancing crack and the microstructure of both variants.

2 | EXPERIMENTAL DETAILS

2.1 | Materials characterisation

The nominal chemical composition of the IN 718 alloy is given in Table 1, confirmed during the present study by energy-dispersive X-ray measurements taken at various random locations. Metallographic sections were prepared from a flow formed and solution heat-treated tube of nominal wall thickness 3 mm, sampled at the mid-wall location. The heat treatment conditions were solution annealed at 980°C for 30 minutes under vacuum before cooling with argon then precipitation hardening at 720°C for 8 hours with subsequent cooling in argon atmosphere for 2 hours. Electron backscattered diffraction (EBSD) inspections were employed as the best means to identify and measure the grain structure. A grain boundary was defined as a local lattice misorientation of >15°. Coincident site lattices were then defined according to the Brandon criteria.[8] A fine scaled and bi-modal

TABLE 1 Nominal chemical composition of IN 718 alloy (wt%)

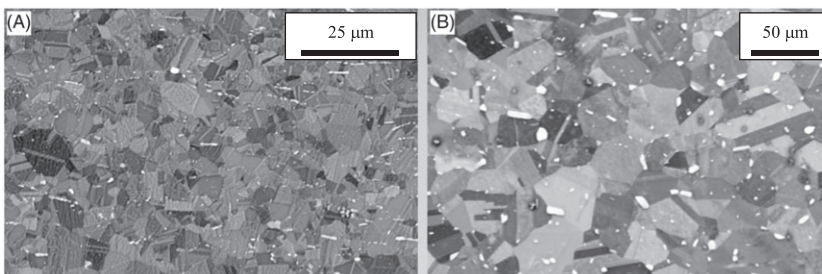| Element	Ni	Cr	Nb	Mo	Ti	Al	Fe
wt%	54.1	18.5	4.6	2.9	1.0	0.6	Bal.

FIGURE 1 Flow formed IN 718 microstructure: A, Fine equi-axed grains. B, Distribution of niobium rich particles

microstructure was evident. The fully recrystallised microstructure (Figure 1A and 1B) contained a random distribution of predominately globular niobium-rich delta phase particles (Ni_3Nb), whereas similar particles in the forged variant tended to be more needle-like in form and often decorated the grain boundaries (Figure 2). An average grain diameter of 3.55 μm was measured in the flow formed variant by using EBSD processing and image analysis software. A 3-dimensional representation of the flow formed microstructure is then compared with the same alloy in the conventional forged and solution heat treatment condition (Figure 3). This illustrates no significant elongation of grains in any direction because of the previous cold work imposed by flow forming, but does define a refinement in grain size (forged = ASTM 7.5 compared with 13.5 for the flow formed).

Detailed EBSD maps indicated no significant difference in the intensity of micro-texture retained in either variant after solution heat treatment and annealing. Focussing on the flow formed variant, however, minor variations in texture were noted through the wall section. Inverse pole figures in Figure 4 demonstrate a preference for 110 planes normal to the Z direction, that is the 110 planes lying parallel to the longitudinal axis of the flow
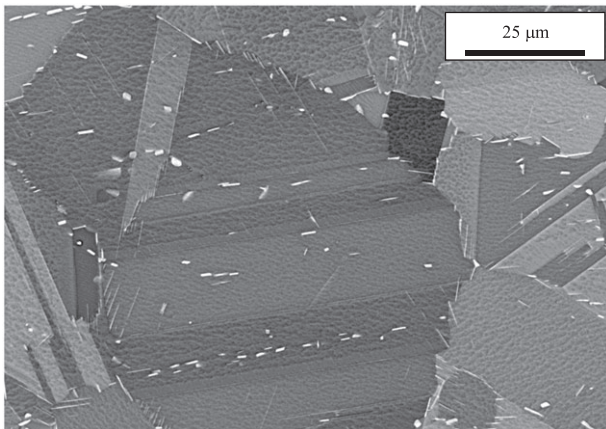

FIGURE 2 Grain boundary and intra-granular distribution of needle-like niobium rich particles in forged variant

formed tube. The intensity of this texture falls from 3.2 times random near the inner tube surface down to 1.3 times random in the mid-wall.

2.2 | Mechanical testing

Mechanical test specimens were extracted parallel to the longitudinal axis of a flow formed tube (Figure 5), retaining the curvature of the original tube across their breadth. The gauge section was profiled by using conventional milling techniques to produce a near rectilinear gauge section of 5 mm in width, with thickness as per the nominal wall thickness of the tube (in this case 2.8 mm). A starter slit was machined by using a diamond tipped slitting tool midway along one inner surface edge of the gauge section. Platinum probe wires of 0.1 mm diameter were spot-welded either side of the slit to enable pulsed, direct current, potential drop measurements of the extending crack (Figure 6A and 6B). In essence, best practice from testing a conventional "corner crack" test specimen was adopted, as normally conducted in this laboratory and described by Mom.[9]

Thus, the inner and outer flow formed tube surfaces were deliberately retained. This would be critical when characterising fatigue strength under low-cycle or high cycle loading conditions (performed but not reported here) since surface condition (ie roughness and residual stress state) could clearly affect crack initiation mechanisms, location, and cyclic life. In the case of the present matrix of crack propagation testing, it was originally considered that surface condition and the minor differences in microstructure at the inner surface when compared with the mid-thickness (see Figures 3 and 4) could also affect behaviour. Any preferential growth along specific faces of the rectilinear section would have developed asymmetric crack profiles rather than quarter circular, part through cracks. Ultimately, as will be illustrated in the results section, this did not appear to be significant.

Cyclic tensile loading was achieved by using bespoke "keep plate" style grips, designed and profiled to interface
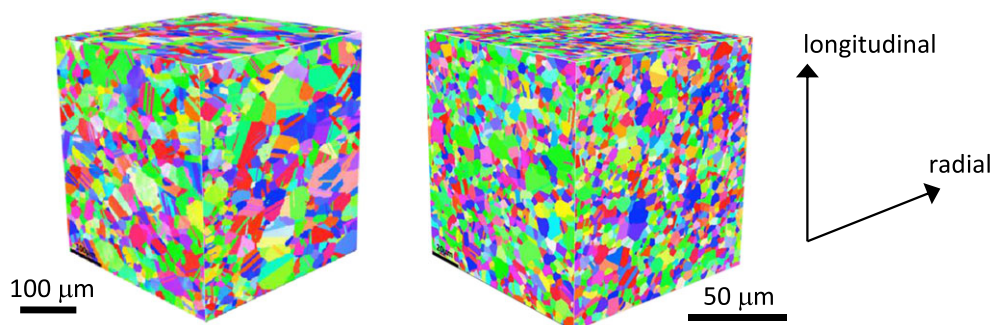

FIGURE 3 Three-dimensional microstructures of IN 718, forged and heat treated (left) and post flow forming and solution heat treatment (right) [Colour figure can be viewed at wileyonlinelibrary.com]
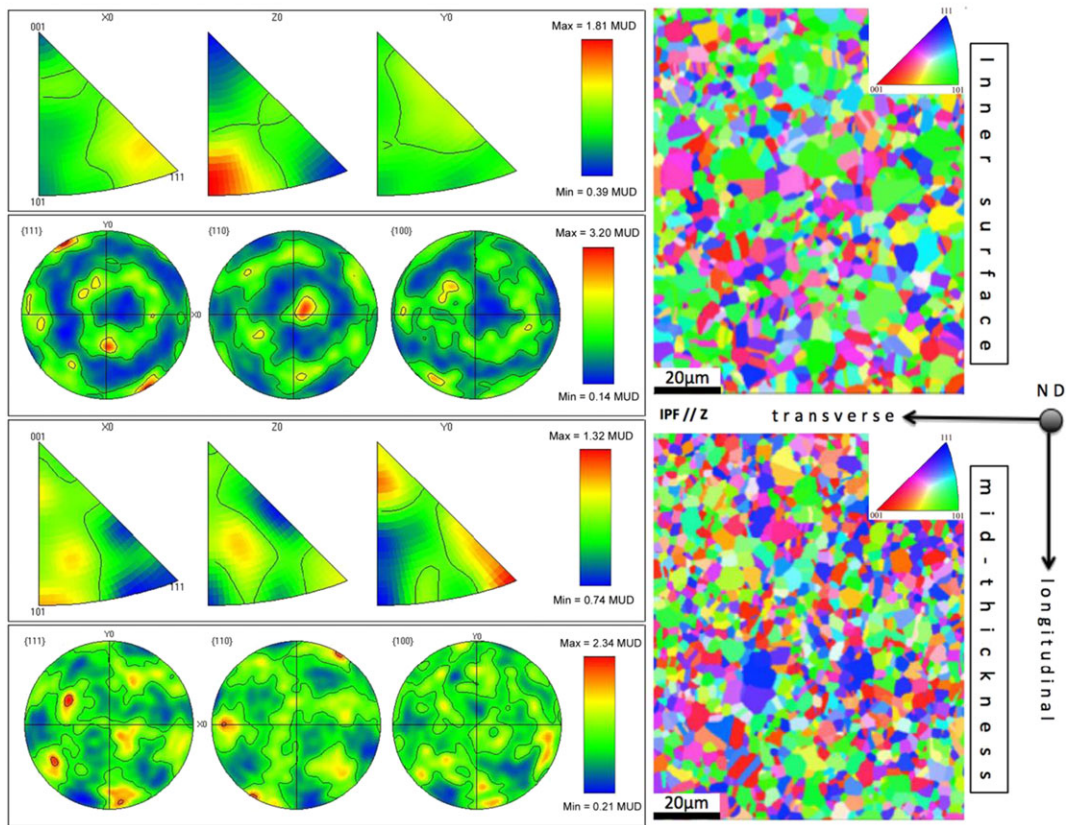
FIGURE 4 Electron backscattered diffraction micro-texture measurements from flow formed material sampled near the inner tube surface and mid wall thickness [Colour figure can be viewed at wileyonlinelibrary.com]
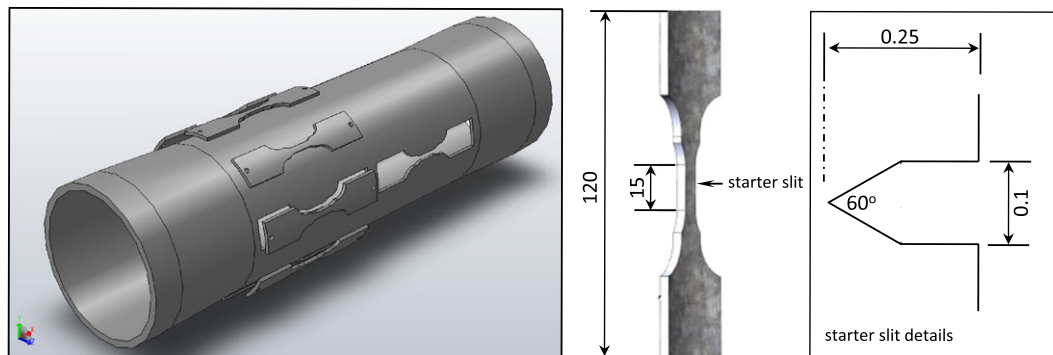

FIGURE 5 Schematic representation of specimen extraction from a flow formed tube, specimen geometry, and detail of starter slit [Colour figure can be viewed at wileyonlinelibrary.com]

with the blend radius and tab ends of the specimen. Constant amplitude load controlled tests were performed to define Paris stage II crack growth characteristics at 20, 300, and 400°C. A trapezoidal, 15 cycles per minute waveform (1 s rise and fall ramps with 1 s holds at peak and minimum load) under $R = 0.1$ was employed for all tests. A stress intensity solution based on a quarter elliptical crack in a rectilinear section was employed, after Newman and Raju.[10] This incorporated data from actual c/w, A/T ratios generated during testing. It was assumed

that the slight curvature to the gauge cross section, inherited from the cylindrical form of the tube, could be ignored. All fractography was performed by using a Zeiss EVOLS25 scanning electron microscope.

Utilising a constant current power supply set to 20 Amps, a linear calibration between the initial crack voltage/length and final crack voltage/length was defined for each individual test, illustrated for a single test in Figure 7A. Automated monitoring of increasing crack voltage with crack extension throughout each test
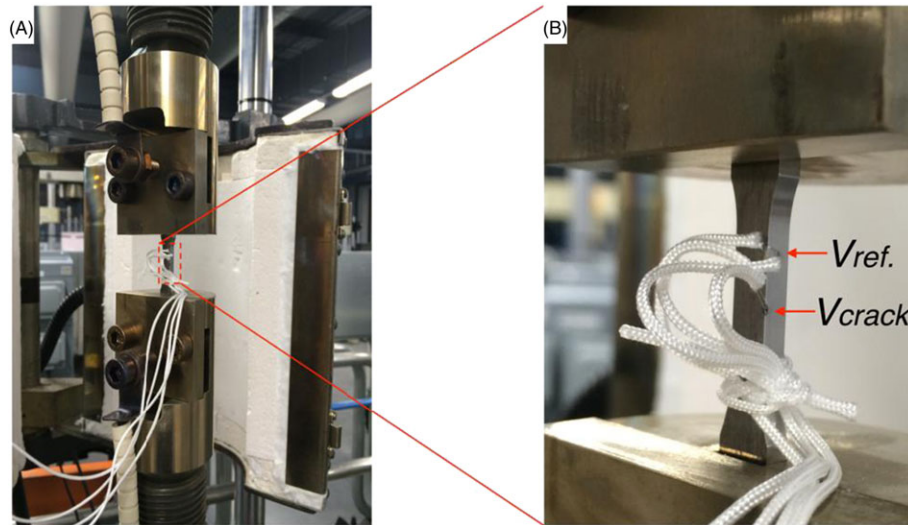
FIGURE 6 A, Bespoke grip design to accommodate specimen curvature. B, Platinum probe wires enabling direct current potential drop measurements [Colour figure can be viewed at wileyonlinelibrary.com]
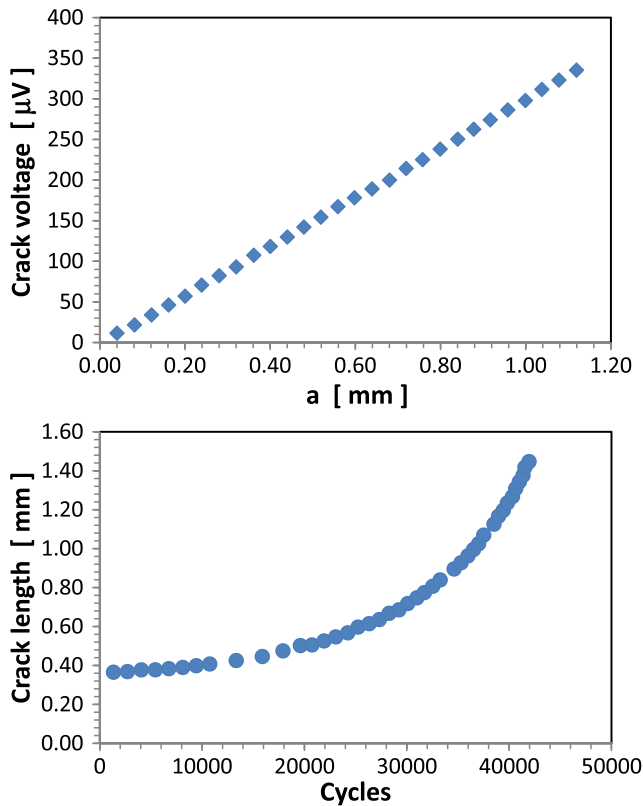

FIGURE 7 A, Examples of crack voltage versus length calibration. B, Crack length versus cycles [Colour figure can be viewed at wileyonlinelibrary.com]

recorded and logged as a function of load cycles, then allowed for conversion of the data into crack length versus cycles (Figure 7B), and ultimately crack growth rates as a function of range in cyclic stress intensity (da/dN versus ΔK). From experience, tests were terminated after

attaining a preset value of crack voltage that ensured that the quarter elliptical crack never exceeded 0.6 of the specimen thickness (ie c/w or $A/T < 0.6$).

For comparison purposes, tests were also performed on identical specimens machined from conventional forged IN 718 material that had been subjected to standard solution and anneal heat treatments. This included inclusion of the curvature to the gauge and tabbed sections.

It was realised from the outset that the volume of the flow formed material available for fatigue characterisation was relatively limited, and given the range of test types required from this variant, there was no opportunity to perform repeat testing to assess variability in the results. Additional campaigns to define static and creep properties were required but not described in this paper. This restriction in the test numbers would eventually be considered during advanced validation programmes once the technique was down selected.

3 | RESULTS AND DISCUSSION

3.1 | Crack growth behaviour

A typical example of crack growth in a flow formed specimen is illustrated in Figure 8. Crack extension from the starter slit has occurred with minimal deviation from the plane orthogonal to the cyclic tensile axis (Figure 8A). When inspected relative to the microstructure, a transgranular mode of growth was confirmed (Figure 8B). High magnification imaging of the crack path confirms the transgranular mode and absence in the influence from the niobium rich particles (Figure 9). The length of the crack growing along the inner flow formed tube
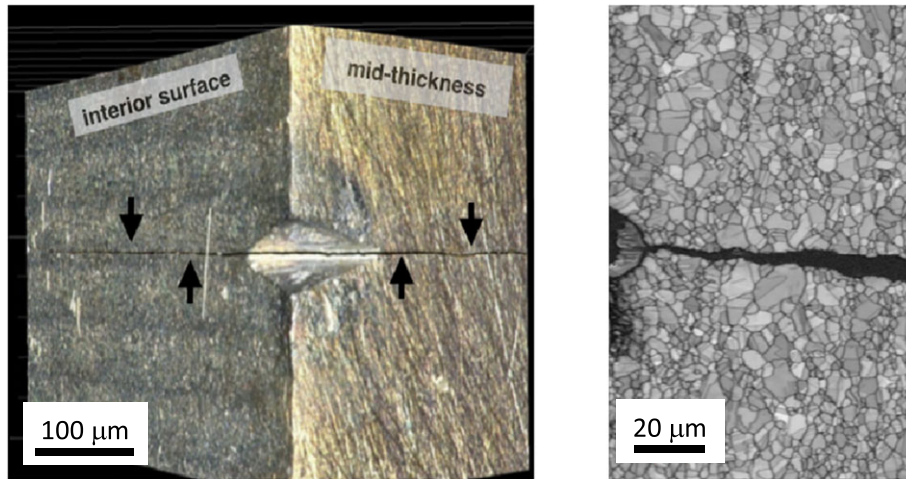
FIGURE 8 Typical crack growth in flow formed IN 718. A, Crack path relative to the interior and through wall thickness surfaces. B, Transgranular crack path away from the starter slit [Colour figure can be viewed at wileyonlinelibrary.com]
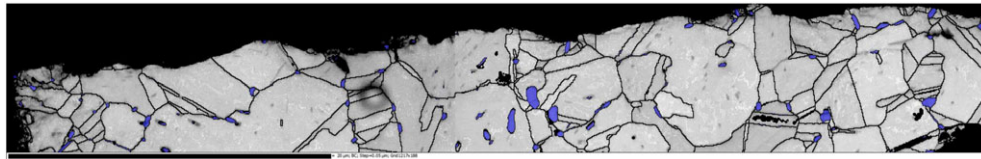

FIGURE 9 Detailed imaging of crack path interactions (fracture surface along top of image) [Colour figure can be viewed at wileyonlinelibrary.com]

surface was near identical to that through the wall thickness; ie a near quarter circular crack profile was produced. This is emphasised in Figure 10A, showing the crack in plane view subsequent to heat tinting and breaking the specimen into 2 halves under a nominal fatigue cycle. Figure 10B then illustrates similar crack morphology in a specimen machined from forged IN 718, further emphasising that flow forming does not appear to influence the profile of the crack. Comparing the 2 macro-scale images, a relatively smoother fracture surface reflects a slightly finer grain structure in the flow formed material. To support our previous assumption that the curvature of the specimen could be ignored from the perspective of stress intensity calculations, it is pertinent to note the essentially rectilinear form of the gauge cross section when sampled on this scale.

Fatigue crack growth data are plotted from 3 tests performed on flow formed specimens (Figure 11A). A minor but consistent increase in crack growth rate was measured at the elevated temperatures of 300 and 400°C compared with 20°C. The coefficients to describe stage II Paris performance are superimposed on the graph. Figure 11B then compares these data to similar experiments on the forged IN 718 variant, with tests conducted under identical conditions. This demonstrates equivalence between the 2 manufacturing processes despite the minor differences in average grain size.

The results from the baseline FCG experiments on flow formed material show that for any given value of ΔK, da/dN increases slightly with increasing temperature between 20 and 400°C. This general trend and magnitude in shift is consistent with previous reports on similar
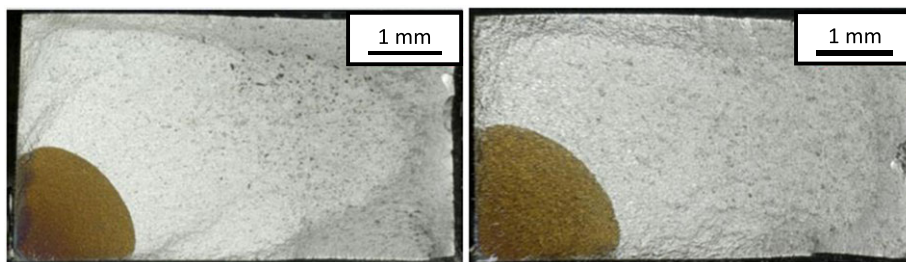

FIGURE 10 Quarter circular cracks in near rectilinear section. (left) Flow formed. (right) Forged [Colour figure can be viewed at wileyonlinelibrary.com]

Test I.D.	m	C	ΔK_{min}	ΔK_{max}
20°C	2.89	7e-12	17.87	28.89
300°C	2.98	7e-12	17.46	28.72
400°C	2.97	1e-11	17.20	27.2

(A)

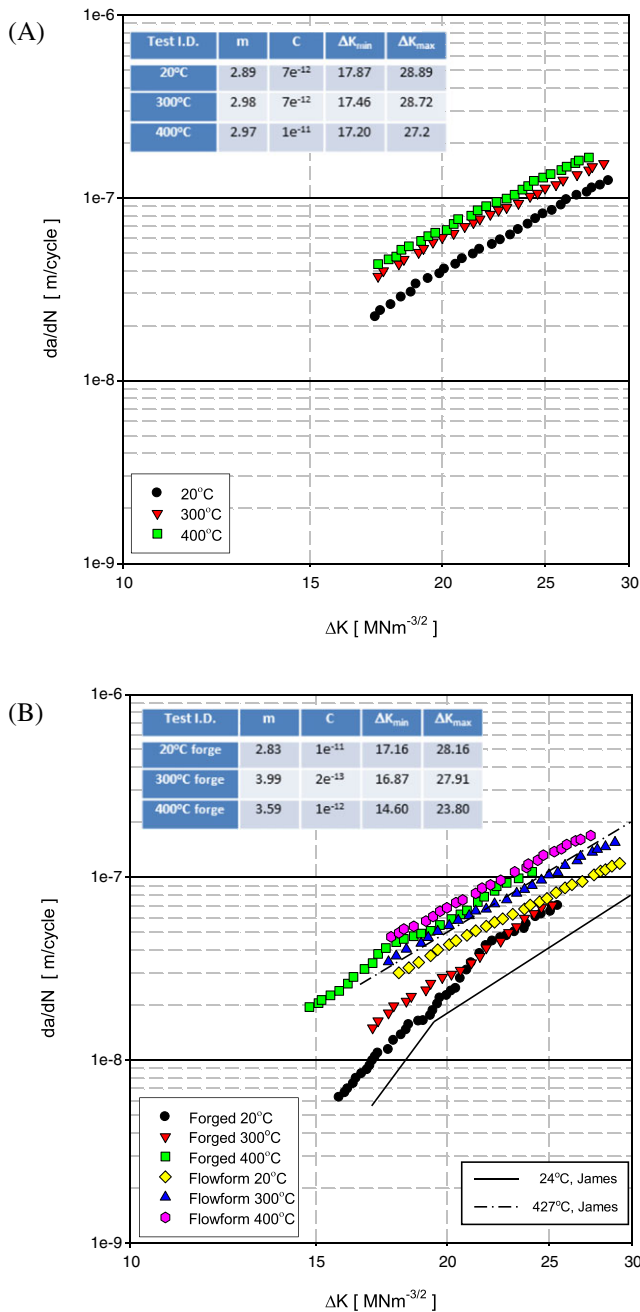| Test I.D.	m	C	ΔK_{min}	ΔK_{max}
20°C forge	2.83	1e-11	17.16	28.16
300°C forge	3.99	2e-13	16.87	27.91
400°C forge	3.59	1e-12	14.60	23.80

(B)

FIGURE 11 A, Fatigue crack growth rate data at 3 different temperatures in flow formed material. B, Comparison between flow formed and forged specimens. All data at $R = 0.1$ [Colour figure can be viewed at wileyonlinelibrary.com]

alloys; for example best fit trends relating to data from James[11] are superimposed in Figure 11B. It may be argued that under low ΔK conditions, the forged IN 718 variant illustrates slightly slower growth rates under test temperatures below 300°C; however, this again was reported by James[11] for a forged variant at room temperature with a distinct break in the Paris slope noted. On the one hand, this could be considered consistent with the classical response to differing grain size (ie coarse grains offering greater FCG resistance). Indeed, James

also went on to show a significant variability in measured growth rates at elevated temperature according to thermo-mechanical processing and grain size in particular. However, it is noted that at higher values of ΔK, the present data sets merge, suggesting that any differences may be due to variation between tests or would fall within experimental scatter should sufficient material have been available for multiple repeat tests. Notably, at the highest temperature bound of 400°C, the data for forged and flow formed variants were virtually identical. This is very encouraging since the flow forming process is yet to be optimised. Any differences between the forged and flow formed variants in measured crack propagation resistance at room and intermediate temperatures will be monitored as the flow forming technique matures.

3.2 | Fractography

Crack growth at all temperatures was dominated by a transgranular mode, epitomised by the specimens tested at room temperature, and illustrated in Figure 12. Faceted growth mechanisms are often reported for nickel alloys tested at lower ΔK regimes (<18 MPa$\sqrt{m}$), whereas striation formation is dominant between 18 and 70 MPa$\sqrt{m}$.[12] During crack growth at low ΔK, where microstructural features will have greatest effect, it has been observed that the majority of crystallographic facets in nickel-based superalloys have a {111} orientation.[13] Flow forming is capable of imparting a significant amount of cold work resulting in a refined grain structure but often elongated in the axial direction. Any residual stress in the microstructure is removed through stress relief or solution annealing. Depending on application, these heat treatments or ageing processes can be optimised to adjust for tensile strength, hardness, and ductility. Clearly, subsequent mechanical properties will be influenced by the degree of cold work and any associated post process heat treatment. A fully recrystallised microstructure with randomly dispersed δ niobium rich particles was noted in the present flow formed material. This was a favourable outcome, since adverse concentrations of δ phase are known to accelerate crack growth rates and have been linked with promoting micro-void nucleation ahead of the advancing crack front.[13]

Under low ΔK conditions, the flow formed specimen in Figure 11A displayed finer scaled facets compared with the relatively larger crystallographic facets seen in the forged variant (Figure 12D). Again, this reflects the difference in grain size. Particle shearing and de-cohesion were observed (Figure 12C) with evidence of slip bands and twining in Figure 12E. The tensile overload regions were characterised by ductile rupture that included micro-void
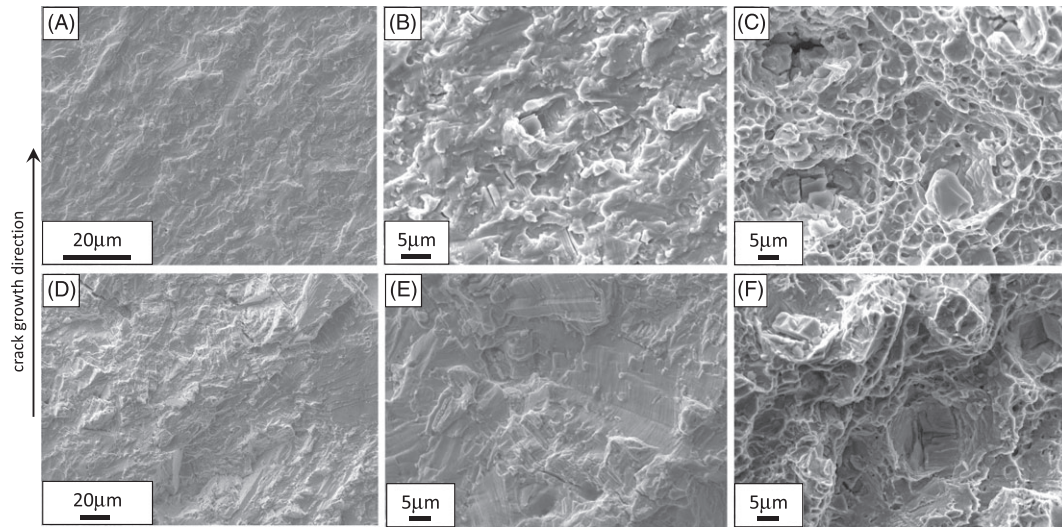
FIGURE 12 Fractographs displaying surface morphology, taken from 3 regions on flow formed (A-C) and forged (D-F) variants, corresponding to low ΔK, mid range ΔK, and overload regimes
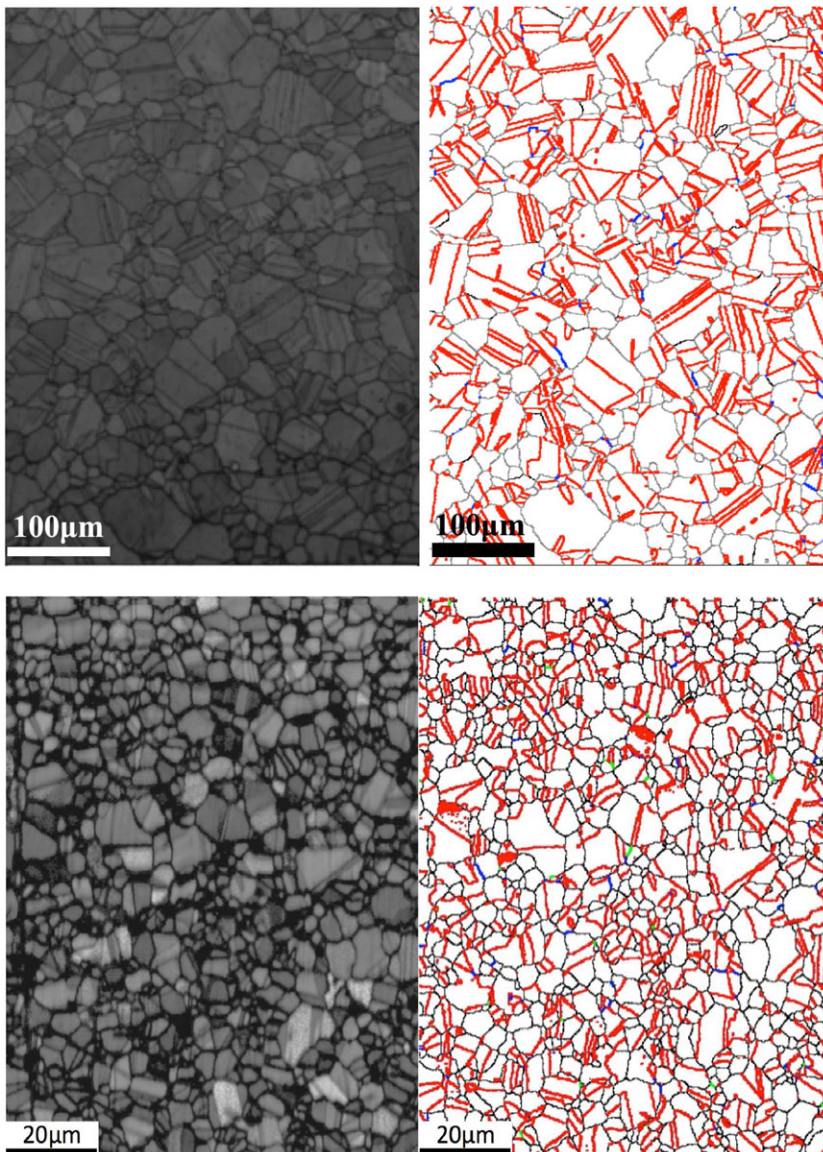

FIGURE 13 Band contrast and coincidence site lattice analysis for forged (top) and flow formed (bottom) variants [Colour figure can be viewed at wileyonlinelibrary.com]

coalescence and evidence of particle shearing/cracking. Energy-dispersive X-ray analysis confirmed the niobium-rich nature of the particles. Such characteristic features were marked in both process variants (eg Figure 12C and 12F).

The distribution of coincident lattice sites associated with low or medium stacking-fault energy was investigated in both variants by using EBSD. Multiple positions sampled along the flow formed tube revealed a microstructure containing 40% of $\Sigma 3$ boundaries by grain boundary length (ie a misorientation of $60 \pm 8.7°$ about the <111>

axis), compared with 55% in the conventional forged counterpart (Figure 13). With an average grain size diameter of 26 μm, the forged material contained a relatively lower percentage of either $\Sigma 9$ (misorientation of $38.94 \pm 5°$ about the <110> axis) and $\Sigma 27$ combined (misorientation of $31.58 \pm 2.89°$ about the 110 axis for "type a" and $35.42 \pm 2.89°$ about the <210> axis for "type b"). Similar populations of $\Sigma 9$ and $\Sigma 27$ were present in the flow formed variant. The $\Sigma 3$ boundaries appear more densely distributed in the flow form materials given the finer grain size emphasised in Figure 14. The inherent relationship
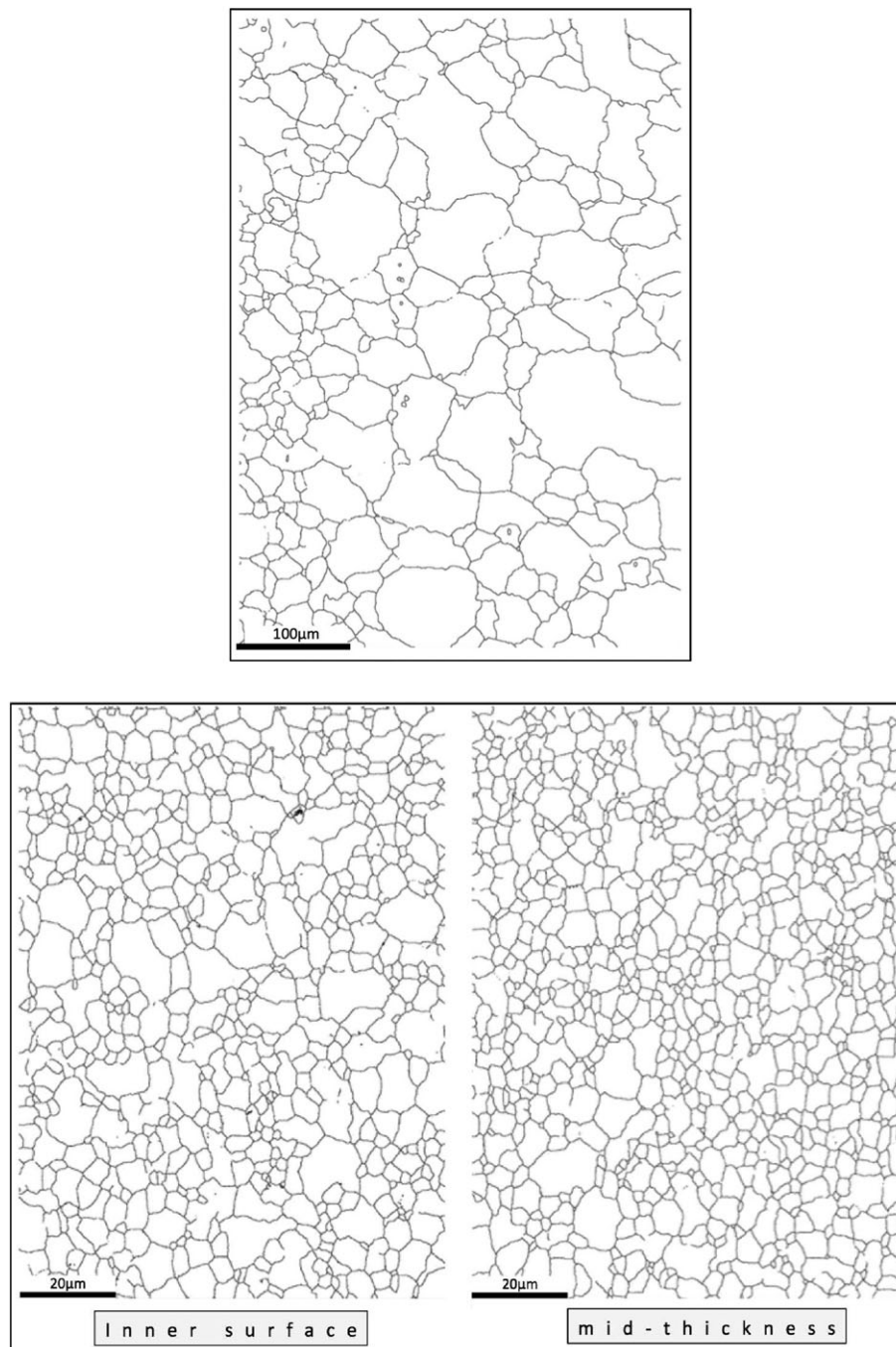

FIGURE 14 Grain boundary connectivity in forged (top) and flow formed (bottom) variants

between grain boundary engineering, thermo-mechanical processing, and optimisation of mechanical properties has been previously discussed in length by Randle,[14] in particular the beneficial effects of $\Sigma 3$ and other "special" boundaries. Araujo et al[15] demonstrated that processing IN 718 via a hot and cold rolling thermo-mechanical route and then annealing below the δ phase solvus temperature to encourage precipitation hardening showed that optimum strength was achieved with a refined microstructure containing a high proportion of $\Sigma 3$, $\Sigma 9$, and $\Sigma 27$. In this study, the influence of flow forming and associated δ phase precipitation on grain refinement produced no adverse effects on twinning mechanism. It is suggested that the predominance of $\Sigma 3$ boundaries in both forms must help accommodate local strain transfer between neighbouring grains and resist any tendency for crack deviation, branching, or intergranular fracture. The equivalence in FCG performance will prove important from the viewpoint of component design and service lifing into the future.

4 | CONCLUSIONS

The following conclusions were drawn from the present study:

- When applied to IN 718, the ambient temperature flow forming process together with the appropriate heat treatment produced a refined equi-axed microstructure with minimal micro-texture.
- Subtle differences in grain size and micro-texture were detected in the flow formed material when comparing the inner tube surface and mid-wall regions.
- A novel technique for specimen extraction and mechanical testing was successfully developed for the assessment of flow formed components.
- Crack propagation behaviour in flow formed IN 178 material demonstrated equivalence to convention forged variants at the extreme of the temperature range assessed (400°C). Any differences noted between the 2 manufacturing routes at 300°C and room temperature will be monitored as the flow forming technique is further optimised.
- Fracture modes were identical in the 2 process variants, scaled according to grain size.

ORCID

M.R. Bache   http://orcid.org/0000-0001-6932-7560

REFERENCES

1. Sivanandini M, Dhami SS, Pabla BS. Flow forming of tubes—a review. *Int J Scientific Eng Res*. 2012;3(5):1-11.
2. Chang S-C, Huang C, Yu S-Y, et al. Tube spinnability of AA2024 and 7075 aluminum. *J Mater Process Technol*. 1998;80–81:676-682.
3. Mohebbi MS, Akbarzadeh A. Experimental study and FEM analysis of redundant strains in flow forming of tubes. *J Mater Process Technol*. 2010;210(2):389-395.
4. Durfee GL. *Adv Mater Process*. 2010;168(10):32-36.
5. Masek B, Malina J, Cerny I, Janicek, S. In: *7th International DAAAM Baltic Conference "INDUSTRIAL ENGINEERING"*, 22--24 April 2010, Tallinn, Estonia.
6. Capdevila C, Chen YL, Lassen NCK, Jones AR, Bhadeshia HKDH. Heterogeneous deformation and recrystallisation of iron base oxide dispersion strengthened PM2000 alloy. *Mater Sci Technol*. 2001;17:693-699.
7. Lee KS, Lu L. A study on the flow forming of cylindrical tubes. *J Mater Process Technol*. 2001;113(1-3):739-742.
8. Brandon D. The structure of high-angle grain boundaries. *Acta Metall*. 1966;14(11):1479-1484.
9. Mom AJA. Revised working document for the AGARD cooperative test programme on titanium alloy engine disc material, AGARD, 1986.
10. Newman JC, Raju IS. NASA Technical Memorandum 85793, NASA, USA, 1984.
11. James LA. In: Loria EA, ed. *Superalloy 718-Metallurgy and Applications*. Warrendale, Pa: The Minerals, Metals & Materials Society; 1989:449-515.
12. Mills WJ, Brown CM. In: *Superalloys 718, 625, 706 and Various Derivatives*, TMS; 2001: 511–522.
13. Duquette D, Gell M. The effect of environment on the mechanism of Stage I fatigue fracture. *Metall. Trans* 1971;2(5):1325-1331.
14. Randle V. Twinning-related grain boundary engineering. *Acta Mater*. 2004;52(14):4067-4081.
15. Araujo LS, dos Santos DS, Godet S, Dille J, Pinto AL, de Almeida LH. Analysis of Grain Boundary Character in a Fine-Grained Nickel-Based Superalloy 718. *J Mater Eng Perform*. 2014;23(11):4130-4135.